Chapter 5

The Impact of Climate Change on Water Availability and Recharge of Aquifers in the Jordan River Basin

Fayez Abdulla, Wim van Veen, Hani Abu Qdais,
Lia van Wesenbeeck and Ben Sonneveld

Additional information is available at the end of the chapter

http://dx.doi.org/10.5772/intechopen.80321

Abstract

Climate change can seriously affect the Middle East region by reduced and erratic rainfall. Formulating appropriate coping policies should account for local effects and changing flows interconnecting spatial units. We apply statistical downscaling techniques of coarse global circulation models to predict future rainfall patterns in the Yarmouk Basin, using a linear regression to extrapolate these results to the entire Jordan River Basin (JRB). Using a detailed water economy model for the JRB we predict rainfall patterns to evaluate the impact of climate change on agriculture and groundwater recharge. For the JRB, rainfall in 2050 will be around 10% lower than present precipitation, but with substantial spatial spreading. An overall reduction of net revenue from crop cultivation is estimated at 150 million USD, with major losses in Israel, Jordan, and the West Bank; Syrian revenues will slightly increase. The recharge of groundwater is affected negatively, and outflow to the Dead Sea is substantially lower, leading to further increases in salinization.

Keywords: Jordan basin, water economy model, climate change

1. Introduction

As is well-known, the current situation in the Jordan River Basin (JRB) is characterized by water scarcity and a history of water-related conflicts. The World Resources Institute (WRI) [1] classifies the JRB riparian countries among the most water-stressed countries in the world with a ratio of withdrawals to supply of more than 80%. Jordan is considered the poorest country in terms of water resources and most of its land is considered to be dry land. Except for the north-western highlands, 90% of the country receives less than 200 mm rainfall per year with an

uneven distribution over regions and high fluctuation from year to year [2]. The population in the JRB region suffers from repeated water shortages which are more severe during the hot summers. Households devote considerable efforts to ensure their daily supply of water. In rural areas, the scarcity of water is among the main difficulties encountered by farmers and in urban areas, tap water is sometimes of bad quality, with frequent shortages. Households are forced to buy bottled or tank water at higher prices for their essential needs.

The severe water-related inequalities [3] are important drivers behind the regional conflicts and have created long-term political instability in the Middle East [4]. Rivalry has persisted over time as an imminent problem that has often been settled through force rather than peaceful cooperation [5]. Individual, uncoordinated actions by all riparian states have resulted in a dramatic change in water flows in the Jordan River Basin. According to United Nations Economic and Social Commission for Western Asia (UN-ESCWA) and Bundesanstalt für Geowissenschaften und Rohstoffe (BGR) [6], annual discharge of water into the Dead Sea under near-natural conditions would be approximately 1300 million m^3, but man-made interventions along the Jordan River and its tributaries have reduced this to 20–200 million m^3 at present. The massive reduction in water availability, particularly in the lower Jordan area, has fueled disputes between the riparian countries. Such disputes continue to obfuscate the relationships between Israel and Lebanon and between Israel and Syria [7]. Looking at the future, prospects for the region seem to be bleak. In the short run, the Syrian crisis with its large regional impact poses a serious threat to livelihoods and development. In the long run, climate change and a rapidly expanding population will continue to put more pressure on water resources.

Climate change is projected to have large impacts on weather patterns across the globe in the future. The Intergovernmental Panel on Climate Change (IPCC) in its 5th Assessment Report (AR5) noted that over the period 1800–2012, the average global temperature increased by 0.85°C. Moreover, Flato et al. [8] indicated that precipitation patterns deviate more frequently from long-term average trends in both volume and erraticism with adverse impacts on the society [9]. Realities of climate change are underpinned by Easterling et al. [10] who related climate change to increased drought incidence, flooding hazards, and reduced biodiversity. This clearly justifies calls for action to mitigate deteriorative effects of climate change. In this study, the focus is on the impact of climate change and water availability for households, effects on recharge to the aquifers, and on economic revenue in the Jordan River Basin, which as was argued above, is an area in the world where water scarcity is a major threat to economic growth and political stability.

Before we come up with practical and well-informed policy solutions, two challenges need to be addressed. First, the low resolution of global climate change models (100–500 km) ignores in-grid variability like complex topographical features and is, therefore, of limited use for impact studies [11]. Second, climate change effects cannot be restricted to changes in rainfall and temperature patterns alone but require a systemic response that accounts for spatial and temporal diversity of the natural resource base, interconnectedness of surface, and subsurface flows and influence on availability of water in volume and quality.

The first issue is addressed by using downscaled precipitation and climate parameters of Abdulla et al. [12] for meteorological stations in the Yarmouk Basin, covering parts of Syria

http://dx.doi.org/10.5772/intechopen.80321

and Jordan. The second challenge is met by using a water economy model of the JRB, which describes the natural and controlled flows in volume and quantity for Jordan River Basin as hydrological entity [13].

The remainder of this chapter is organized as follows. Section 2 gives a brief description of the structure, empirical basis, and calibration of the JRB water economy model. Section 3 presents the scenario formulation, including downscaling. Section 4 reports on the impact of climate change and Section 5 concludes and indicates pathways for further research.

2. The Jordan River Basin (JRB) model

Theoretically, the JRB model is a special case of the general class of welfare optimization models [13], where the innovative part is the inclusion of hydrology as central component of the production technology. Hence, control of flows (extraction of groundwater; use of water by humans; animals; and agriculture; transfer of water through canals; wastewater treatment and desalinization) conforms to basic principles of microeconomics with constraints that respect conservation. For economics, this implies that commodity balances hold; for hydrology, mass balances for pure water as well as for pollutants dissolved in water are maintained.

In its representation of the water economy of the JRB, the model distinguishes 48 districts, and 26 (two-weekly) time steps. Water can flow within and between five different layers. These comprise a surface layer on land for natural flows, a surface layer on land representing anthropogenic influences on water, a river layer, a root zone, and a layer representing the aquifer zones in the basin. Finally, next to clean water, the model can accommodate three types of pollutants: salinity, biological oxygen demand (BOD), and nitrate. The combination of place, time, layer, and quality defines a "cell" within the model, which acts as a source and destination of flows, representing the high level of interconnectedness of flows within the JRB.

2.1. Schematic representation of flows within the model

Figure 1 provides a schematic overview of flows within the JRB between the main layers, as well as flows entering the basin as whole (rainfall and lateral flows from outside the basin) or leaving the basin (evaporation, lateral flows leaving the basin). In the model, each of the layers and connections with other layers is modeled in detail, following hydrological laws as well as reflecting anthropogenic activity (pumping, irrigation, use by humans, livestock, industry and municipalities, sewage, waste water treatment and reuse, and water harvesting).

2.2. Water quality

As mentioned before, the JRB water economy model represents pollution of three specific types —salinity, nitrate, and BOD. Instead of using a set of attributes to represent water quality in each of these three dimensions at each point in time and space, the model represents these pollutants as flows, for which balances must hold, as for pure water. Hence, conceptually, pollutants are represented as flows with standard concentrations: 25 g/l for Cl, 2 g/l for NO_3, and 10 g/l for

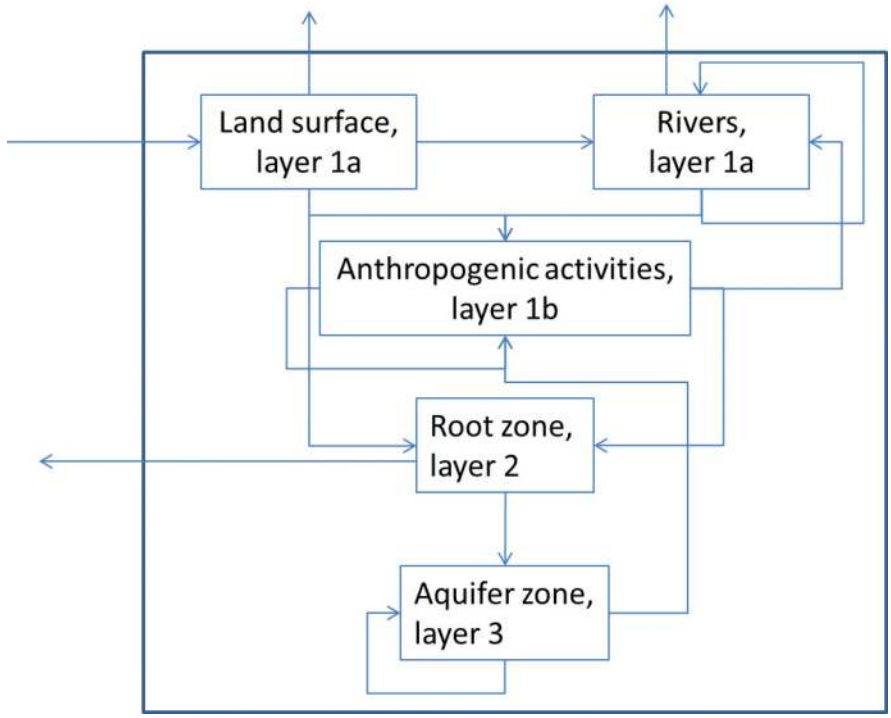

Figure 1. Schematic overview of flows within the JRB basin.

BOD. Observed concentrations are obtained by mixing the volumes of these flows with the volume of pure water. However, such a separation of flows would not do justice to the fact that pollutants flow with the water, and are not separable in reality. Hence, in the model application, flows are always combined. Where water quality changes, this is explicitly represented as a production process (water treatment) or a natural process (decreased quality through the uptake of pollutants from the soil). Consumers, livestock, and plants (irrigation) have to take the quality of water as it is at the location where it is offered, and this represents the channel through which quality changes enter into the system and affect yields, quality of produce and revenue.

2.3. Schematic representation of farmer behavior

Given the overriding importance of agriculture as economic activity in the JRB, the focus in assessing economic impact is on agriculture. In the JRB, crop cultivation is characterized by a dual system, where irrigation-based agriculture and rain-fed agriculture both exist. Hence, in principle, each farmer may have both types of land under cultivation. If profit maximization is taken as point of departure, a farmer in principle controls: (1) the amount of land under cultivation, (2) the share of the land that is irrigated, and (3) the crop(s) cultivated. In its simplest interpretation, profit maximization would be driven by the amount of water available for irrigation; the costs of inputs as well as irrigation water; and the output prices of different crops, while constraints would be defined by the response of different crops to the supply of water and other inputs.

http://dx.doi.org/10.5772/intechopen.80321

The water response module of the model is richer than this simple representation, but also imposes some simplifying assumptions. To start with the latter, it is assumed that the crop composition observed in the base year 2010 is maintained under changing water availability. Furthermore, prices for inputs, water, and crops are assumed to remain constant, as are costs for irrigation. Richness of the module is achieved by acknowledging the following facts of agriculture in the JRB:

1. Whenever land is irrigated, irrigation applied is optimal for the crop under cultivation
2. Quality of land is not uniform over the JRB or even within districts
3. The highest-quality land is taken into production first; then, lesser qualities are used for cultivation
4. Water available for irrigation may contain (high levels of) salt, BOD, or nitrate
5. There is a large gap between yields on irrigated lands and yields on rain-fed areas
6. Yields on rain-fed areas mainly respond to changes in water availability
7. The area of rain-fed land does not respond to changes in water availability

This results in a decision tree for the farmer as depicted in **Figure 2**. For rain-fed lands, the farmer has no control over the response, as water availability in the root zone as well as water quality determine the yield on the given area. For irrigated lands, the farmer controls the area under irrigation (this block is marked purple, to indicate this is a decision variable). Yield response for the total area under irrigation is the result of expansion of irrigated areas to include land of lesser quality, where the optimal yield under irrigation is lower, leading to lower average yields for the total irrigated area. As for rain-fed agriculture, salinity has a negative impact on crop yields, and hence, also impacts on the yield response. Below, the chapter expands on the formal description of the water response module.

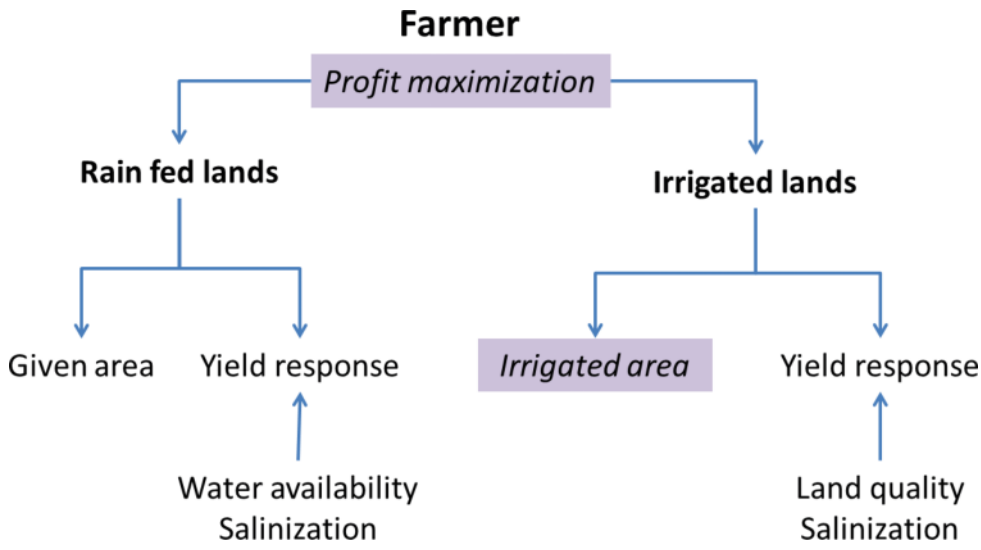

Figure 2. Farmer's response to changes in water quality and quantity.

2.4. Specification of the simulation model

Formally, the model can be represented by the following four equations:

$$d^i = \Delta^i x \tag{1}$$

$$e^j = H^j x \tag{2}$$

$$\tilde{x} = Rx \tag{3}$$

$$\sum_i d^i + \sum_j e^j + \tilde{x} = A\tilde{x} + \sum_i B^{0i} d^i + \sum_j B^j e^j + b \tag{4}$$

where b is the exogenous water availability (net rainfall, springs), d^i is water use of demand type i, e^j denotes input of project j, x represents water stock, $\tilde{x}$ is water volume available for natural outflow (including retention) and t represents time (two-weekly periods), while indices h are water quality classes, s are locations (district, river segment), ℓ are soil layers, i represents the type of water use and j the type of project. Finally, the following matrices of coefficients are defined in the model: A; the matrix of natural flow coefficients, B^{0i}; the matrix of return coefficients of demand type i, B^j; the matrix of return coefficients of project j; and Δ^i, a diagonal matrix with elements δ^i; H^j, a diagonal matrix with elements η^j; and R, a diagonal matrix with elements ρ.

Eq. (4) shows for each (h, s, t, ℓ) the balance between the destinations of the available water stock and the origins of this stock. Destinations are on the left-hand side, consisting of human water use, water inputs in projects and natural outflow. The latter includes retention, i.e., water of quality h remains at the same (s, ℓ) from t to $t + 1$. Origins of water availability are on the right-hand side, consisting of natural inflows, return flows from water use, return flows from projects, and exogenous availability from rainfall and springs.

Eqs. 1–3 specify each of the destinations as fixed fractions of the total available model stock x. Since retention is part of the natural outflows, the fractions logically have to add to one. Furthermore, the fractions have to reflect one important restriction, viz. that the user has to accept the quality of the available stock x. Therefore, the fractions do not depend on index h. More precisely, (1)–(3) can be written as:

$$d^i_{hst\ell} = \delta^i_{st\ell} \;\; x_{hst\ell} \tag{5}$$

$$e^j_{hst\ell} = \eta^j_{st\ell} \;\; x_{hst\ell} \tag{6}$$

$$\tilde{x}_{hst\ell} = \rho_{st\ell} \;\; x_{hst\ell} \tag{7}$$

2.5. Coverage of water flows

Although the equations look relatively simple, they cover a wealth of different flows especially due to the dimensionality of the system. We distinguish a hydrological component, anthropogenic activities, and actual human water use.

http://dx.doi.org/10.5772/intechopen.80321

The hydrological component is represented by matrix A. Element $A_{hst\ell,h's't'\ell'}$ of matrix A denotes the share of $\tilde{x}_{h's't'\ell'}$ that flows in a natural way to (h,s,t,ℓ). Logically, the sum of these shares should not exceed one. In this way, the model can represent flows such as run-off of rainwater to the river system, percolation of rainwater to the root zone and further down to the groundwater zone, downstream flows from one river segment to the other or into Lake Tiberias, and retention of water at the same location and layer. Whenever relevant, changes in quality are also captured in this way, for instance taking up nitrate from the soil in run-off and percolation. If the sum of the outflow coefficients is less than one, it means that water disappears from the JRB. One may think in particular of evaporation or outflow to the Dead Sea. In the last period $(t = T)$, water disappears also via retention (becoming available next year).

In addition to these natural flows, the model has exogenous natural flows denoted as vector b. This parameter covers both net rainfall and water from springs. Net rainfall is measured after subtraction of immediate evaporation. It is important to be precise in this respect since immediate evaporation amounts to more than 10% of gross rainfall for the JRB as a whole. Spring water is essentially transferred from the groundwater zone to the surface zone of the district where it is used or to the river segment that it feeds. Hence, it has negative and positive values, summing to zero. For the first period $(t = 1)$, parameter b also covers the initial stock retained from the previous year.

Anthropogenic activities are represented by several projects j: groundwater pumping, rainwater harvesting, river outlets (dams), surface water transfer (canals, carriers), and irrigation. The input volumes of these projects are given by vectors e^j, each with dimensions $h,\ s,\ t, \ell$. The impact of the project is measured by elements $B^j_{hst\ell,h's't'\ell'}$, representing output (h,s,t,ℓ) per unit of input $\left(h',s',t',\ell'\right)$. Projects that merely transfer water have allocation shares to a different layer or location (or period, in case of lags) for the same quality h. If water quality changes too, there are also allocation shares to quality classes $h' \neq h$. Just as for matrix A, the sum of the output coefficients should not exceed one. Again, a sum strictly less than one means that water is disappearing from the JRB (evaporation, carrier to outside). Losses and leakages of projects are booked as output to other layers than intended, including evaporation.

Five types of water use are distinguished: household use, municipal use, industrial use, crop water use, and livestock use. Household water is further subdivided into tap water, truck water, roof water, and bottled water. Together, these destinations make up the set of water use types i. The public water distribution system delivers household tap water, municipal water, and industrial water. Eq. (1) specifies each type of water use as fraction of the available water stock. Therefore, d^i indicates gross water use, before purification.

When strictly following its definition above, matrix B^{0i} represents merely the return flows of used water, with element $B^{0i}_{h\ s\ t\ \ell,h's't'\ell'}$ denoting the return volume of (h,s,t,ℓ) per unit of water use $\left(h',s',t',\ell'\right)$. However, since d^i indicates gross water use, matrix B^{0i} covers in fact a chain of activities: (a) water purification and distribution, (b) the actual return flow (production of waste water), (c) sewerage (collection of waste water), and (d) treatment of waste water.

To this, we may add even transport of raw and treated waste water. Hence, matrix B^{0i} is a composite of several matrices, although the number may differ across types of use i. Still, for B^{0i} the same condition as for A and B^j holds, viz. that the sum of its output coefficients should not exceed one. Distribution leakages and waste water dumping are booked as output to other layers than intended and where local quality changes result, this is also modeled as a pollution process.

2.6. Properties of the model

Here, we summarize the main properties of the model:

i. *No water creation:*

- for each (h, s, t, ℓ), the sum of the natural outflow coefficients does not exceed one
- for each (h, s, t, ℓ) and each project j, the sum of the project return coefficients does not exceed one
- for each (h, s, t, ℓ) and each type of use i, the sum of the demand return coefficients does not exceed one

ii. *Stock-driven flows:* all endogenous natural flows, all project inputs, and all volumes of water use are specified relative to the total available water stock

iii. *Blending property:* all users have to accept the quality of the available water stock; hence the fixed fractions in Eqs. (5)–(7) are independent of water quality class h

iv. *Exhaustive allocation of outflows*: the sum of the fixed fractions of all destinations, including those outside the JRB, is equal to one.

In model symbols the latter condition reads:

$$\sum\nolimits_i \delta^i_{st\ell} + \sum\nolimits_j \eta^j_{st\ell} + \rho_{st\ell} = 1 \tag{8}$$

Due to this condition, we can write Eq. (4) also fully in terms of total available stock x:

$$x = ARx + \sum\nolimits_i B^{0i}\Delta^i x + \sum\nolimits_j B^j H^j x + b \tag{9}$$

This formulation is used in the iterative calculation of the equilibrium stock levels that solve the model, starting from an initial value, say $x = x^0$. Due to the property of "no water creation," Eq. (9) represents a contraction mapping. Together with non-negativity of the parameters, this contraction property ensures convergence of the iterative calculations to a unique, non-negative fixed point x^*. The definition of a contraction mapping and the proof of this proposition are given in Chapter 6 of Keyzer[1] [14].

[1]In actual applications, this result will also hold if some of the elements of b are negative, provided that these negative values are overruled by other large positive values on the right-hand side of Eq. (6).

2.6.1. Crop revenue

Once the equilibrium stock x^* has been obtained, the corresponding values of d^i, e^j, and $\tilde{x}$ can also be calculated, including crop water use, taken up from the root zone, distinguished by location s, period t, and quality h. Based on the outcomes for crop water use, the impact on the net revenue of the farmer is calculated using additional exogenous information on the crop production structure in each district. This impact reflects both the direct impact of water on crop yields and the reaction of the farmer to the changes in water availability and water quality.

To this end, the simulation model includes a crop module that distinguishes K different crops, indexed k, and two land types, indexed m, viz. irrigated land (with or without protection) and rain-fed land. Water use and crop yields per hectare are different across these two land types. We introduce the following notation.

a_{kms} denotes harvested area of crop k on land type m in district s, per calendar year, in ha; $\overline{a}_{kms}$ is the reference area of crop k on land type m in district s, per calendar year, in ha; w_{kmhs} is the water use of quality h by crop k on land type m in district s, per calendar year, in m^3/ha; y_{kms} is the yield of crop k on land type m in district s, per calendar year, in kg/ha; $\overline{y}_{kms}$ is the reference yield of crop k on land type m in district s, per calendar year, in kg/ha; r_{kms} is net revenue of crop k on land type m in district s, per calendar year, in USD/ha; u_{kms} are the input costs (other than water) for crop k on land type in district s, per calendar year, in USD/ha; p^f_{ks} is the farm gate price of crop k in district s, in USD/kg; p^w_s is the water price paid by crop farmers in district s, in USD/m^3; and ρ_s is total net revenue from cropping in district s, per calendar year, in USD. The reference areas and yields refer to the observed 2010 levels.

Net revenue is calculated as follows:

$$r_{kms} = p^f_{ks} y_{kms} - u_{kms} - p^w_s \sum_h w_{kmhs} \tag{10}$$

$$\rho_s = \sum_{k,m} r_{kms} a_{kms} \tag{11}$$

The relation between actual harvested area a_{kms} and reference area $\overline{a}_{kms}$ and the relation between actual yield y_{kms} and reference yield $\overline{y}_{kms}$ are described by, respectively:

$$a_{kms} = \alpha_{kms} \ \overline{a}_{kms} \tag{12}$$

$$y_{kms} = \beta_{kms} \ \left(\gamma_{kms}/\overline{\gamma}_{kms}\right) \ \overline{y}_{kms} \tag{13}$$

In Eq. (12), α_{kms} represents the area adjustment due to the changes in water availability, expressed as factor relative to the reference area. For irrigated area, the factor depends positively on the water availability, irrespective of water quality. Depending on this volume, the factor is larger or smaller than one. For rain-fed area, the factor is by definition equal to one, hence no adjustment.

In Eq. (13), β_{kms} represents the yield adjustment factor due to changes in the availability of total water (irrespective of quality) while $\gamma_{kms}/\overline{\gamma}_{kms}$ measures the impact of changes in salinity. For

irrigated area, factor β_{kms} is determined simultaneously with factor α_{kms} in (12), based on a subdivision of potentially irrigable land in land suitability classes. In case of extension of irrigated land, the factor may decline. For rain-fed area, factor β_{kms} is directly and positively related to water availability. Hence, for both land types, β_{kms} can be larger than or smaller than one.

Factor γ_{kms} measures the yield effect of salinity. It is calculated as a declining, piecewise linear function of the salinity level. By standardizing it to the 2010 reference value $\overline{\gamma}_{kms}$, the salinity impact in (13) is also a factor that can be larger than or smaller than one, just as factor β_{kms}.

In these equations, prices p^f_{ks} and p^w_s are exogenous, and so are reference areas $\overline{a}_{kms}$, reference yields $\overline{y}_{kms}$, and input costs u_{kms}, whereas factors α_{kms}, β_{kms}, and γ_{kms} depend on water volumes w_{kmhs}. Merbis and Sonneveld [15] describe the specification of these factors in more detail.

3. Scenario formulation

The following steps were taken to evaluate climate change impacts. First, we organized the daily precipitation data of the five climate change scenarios over the period 1980–2100 for 23 stations in the Yarmouk Basin in a excel spread sheet. Second, since variety of the modeled data are difficult to compare at daily level, we aggregated precipitation at yearly level and averaged the data of individual stations over cohorts of 20 consecutive years (2000–2020, 2021–2040, etc.) for each district. Third, we calculated relative changes over 40 (average of 2000–2020 minus 2040–2060) and 80 (average of 2000–2020 minus 2080–2100) years (**Table 1**). Fourth, using a linear regression that estimated a small positive gradient for the northern latitude [16], the predicted rainfall patterns for the Yarmouk river basin have been extrapolated to the entire JRB, constituting a database for the scenario analysis of daily rainfall at district level for the year 2050 (regression results are found in the Annex). Finally, we selected the CanESM2 model since, here, grid of the model overlaid best with the JRB area (in particular, better than CGCM3, see **Figure 3**); within CanESM2, RCP8.5 is selected as the most pessimistic scenario on future rainfall.

District	Altitude	North	Climann1_40	Climann2_40	Climann3_40	Climann4_40	Climann5_40	Climann1_80	Climann2_80	Climann3_80	Climann4_80	Climann5_80
CN21001	780	32,045	0,08	0,13	0,16	0,29	0,34	0,19	0,19	0,33	0,41	0,47
CN22021	-218	32,103	0,11	0,13	0,15	0,34	0,41	0,22	0,16	0,32	0,50	0,58
CN21010	715	32,299	0,08	0,20		0,43	0,46	0,21	0,25		0,51	0,56
CN21005	709	32,332	0,06	0,12	0,16	0,28	0,32	0,20	0,18	0,30	0,36	0,42
CN41004	1090	32,616	0,06	0,16	0,14	0,15	0,17	0,16	0,20	0,39	0,32	0,37
CN41007	618	32,791	0,06	0,14	0,12	0,09	0,09	0,16	0,18	0,31	0,22	0,28

Climann1_ = CanESM2 GCM, RCP2.6, **Climann2_** = CanESM2 GCM, RCP4.5, **Climann3_** = CanESM2 GCM, RCP8.5, **Climann4_** = CGCM3 GCM, A1B, **Climann5_** = CGCM3 GCM, A2. **-40** = 40 years of difference, **_80** = 80 years of difference.

Table 1. Relative changes in annual precipitation by climate change scenario.

http://dx.doi.org/10.5772/intechopen.80321

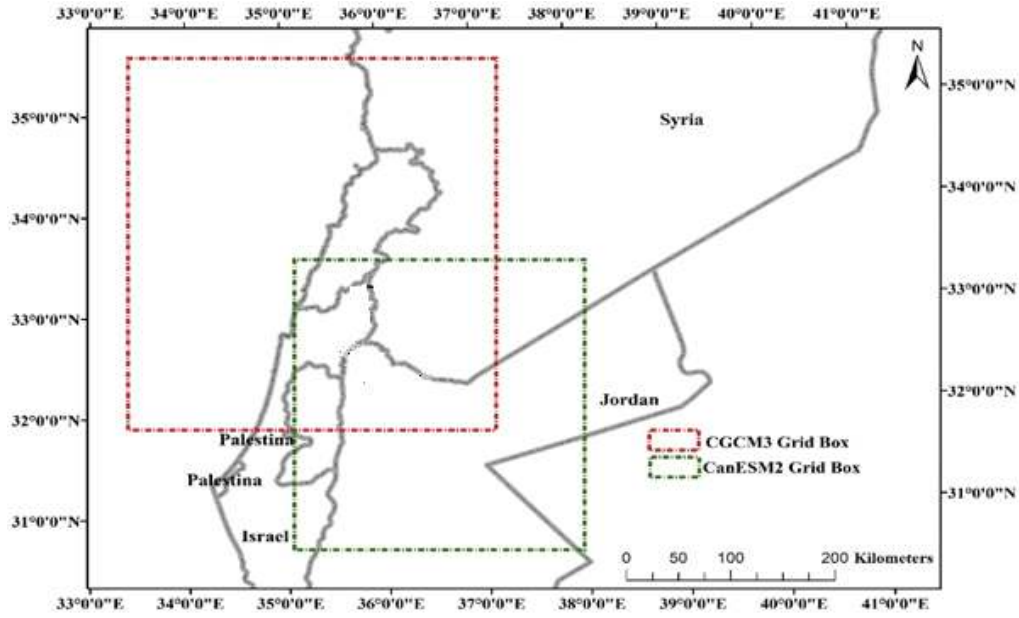

Figure 3. Grid overlay of CanESM2 and CGCM3 with JRB.

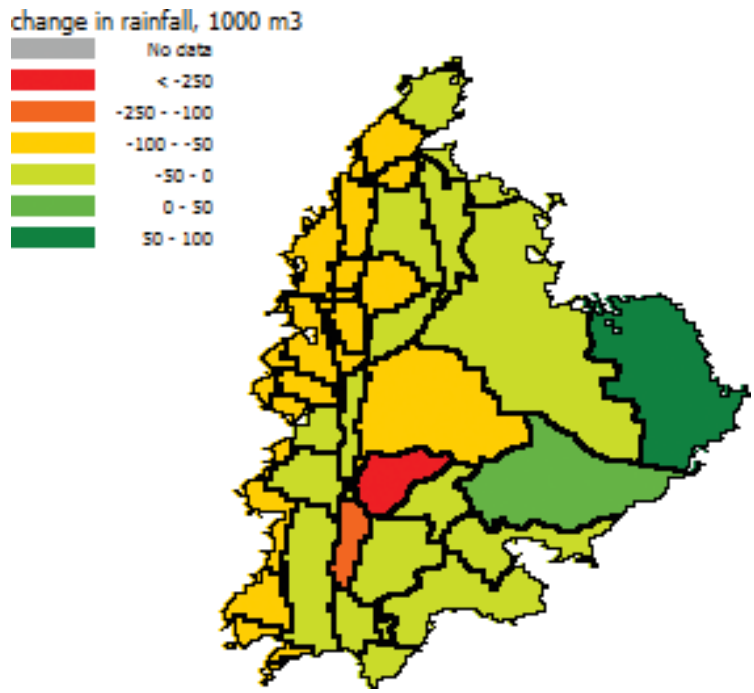

Figure 4. Rainfall in 2050: Predicted change relative to present conditions.

Following this procedure, we predict that for the whole of the JRB, rainfall in 2050 will be around 10% lower than present precipitation, but with substantial spatial spreading (see **Figure 4**), where rainfall is even predicted to increase in the eastern part of the JRB.

4. Impact of climate change

Application of the JRB model using these rainfall figures leads to the conclusion that the most important impact is an overall reduction of the net revenue from crop cultivation in the JRB as a whole of 150 million USD, with major losses in Israel, Jordan, and the West Bank. Syrian revenues would increase, reflecting the increase in rainfall in large parts of the country located in the JRB (see **Figure 5**).

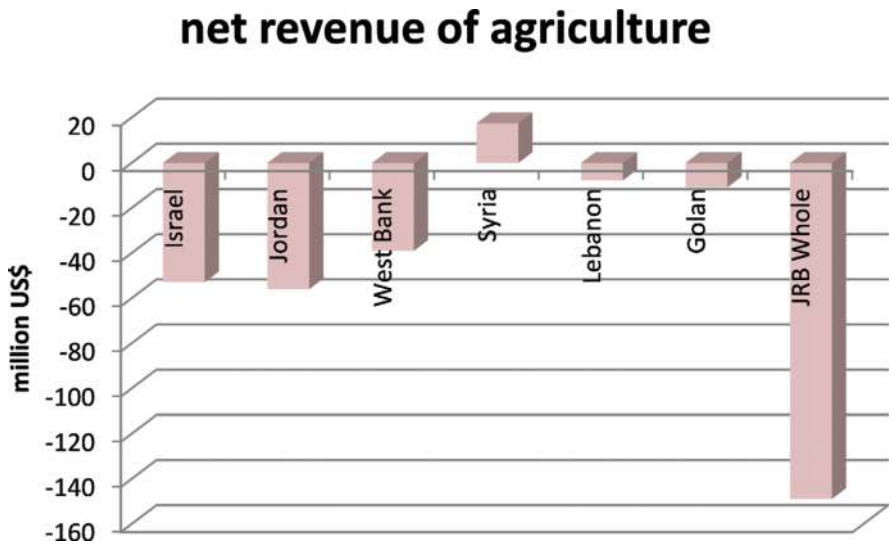

Figure 5. Impact of climate change on net revenue.

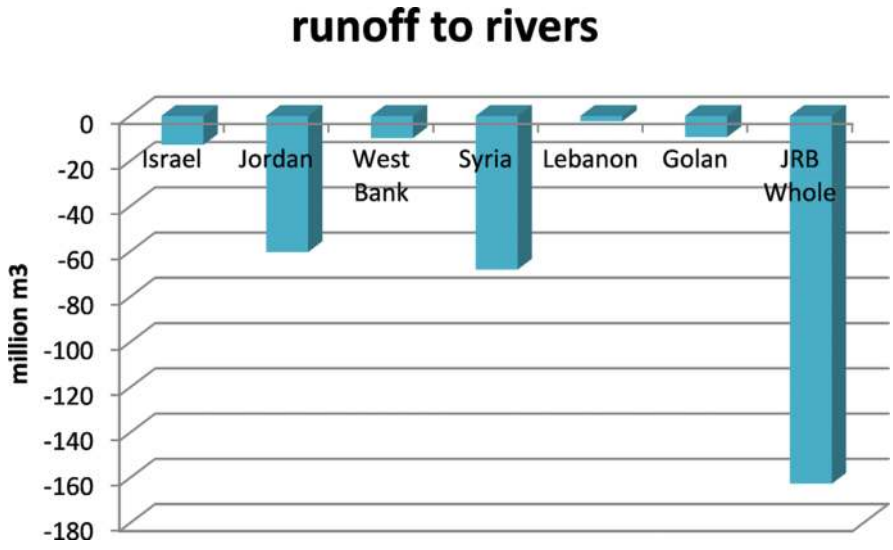

Figure 6. Impact of climate change on run-off.

http://dx.doi.org/10.5772/intechopen.80321

However, the rainfall shock is not fully transmitted to agricultural activity: although the reduction in rainfall is a major shock, it is partly compensated by reduced evaporation (about half the shock), and lower river flows and hence lower extraction volumes. In addition, recharge of groundwater is affected very negatively, and the outflow to the Dead Sea is also substantially lower (20 million km^3). Despite the drop in recharge, salinity of groundwater resources increases only marginally (0.01% for the JRB as a whole, with a "peak" of 0.02% for Israel). Decreasing availability of water implies a decrease in the amount of untreated waste water, as household

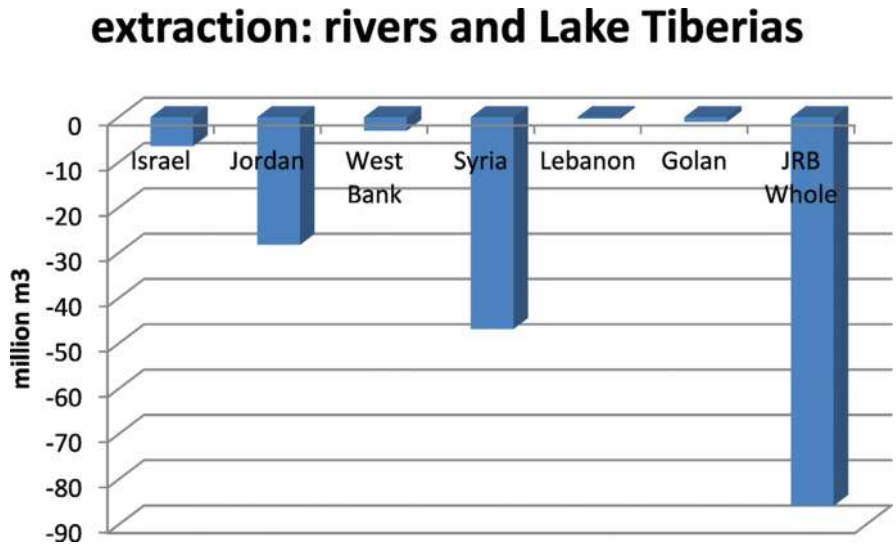

Figure 7. Impact of climate change on extraction.

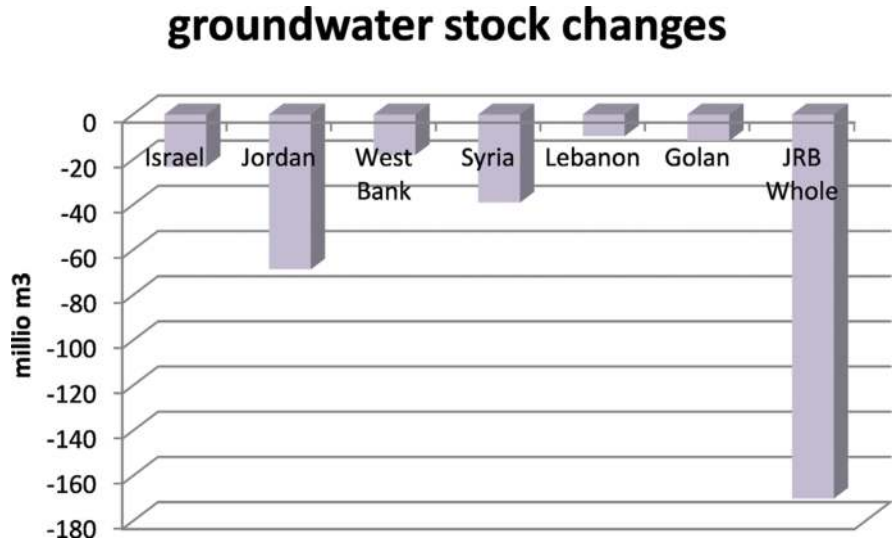

Figure 8. Impact of climate change on groundwater stock changes.

demand falls and less waste water is produced. This in turn implies that irrigation water contains relatively less untreated waste water and that leakage of contaminated water to the root zone also decreases, leading to a reduction in BOD in water used for irrigation of 5.5% on average for the JRB. **Figures 6–8** illustrate the impact on run-off to the rivers, extraction from the rivers and Lake Tiberias and groundwater stock changes relative to the present baseline. Particularly, the latter result is cause for concern about the future as it is clear that unchanged extraction policies would lead to unsustainable extraction from groundwater resources in the coming decade.

5. Conclusions and way forward

Climate change is a major concern for policy makers in the Middle East who aim to protect their constituency from adverse effects on water availability for food security and the environment. Yet, to provide a proper foundation for informed decisions on adoption or mitigation of climate change effects, two issues have to be resolved. First, results of global circulation models should be downscaled from their coarse (50–100 km) grids to a meaningful spatial resolution. Second, effects of changes in rainfall should reflect the hydrological complexity of natural and controlled surface and subsurface flows that jointly are responsible for water supply.

In this study, we addressed these two issues for the JRB by a statistical downscaling of the climate change scenarios for precipitation from global circulation models in conjunction with the application of a water economy model that describes the water flows in detail and, additionally, reports on the impact of climate change on water availability (run-off and groundwater recharge) and agricultural productivity in JRB.

The results reveal that there is a significant reduction in the surface run-off of an amount greater than 160 MCM (28%) in the JRB that affects the extraction volumes out of the rivers. Most reduction in run-off to rivers is found in Syria (42%) and Jordan (40%). There is also a significant reduction in groundwater recharge of an amount of about 180 MCM (11%), which seriously threatens the already overexploited groundwater stock. Accordingly, the agricultural productivity reduces by 160 million USD, with largest effects on Jordan (23%), the West Bank (16%), and Israel (12%). The impact of climate change on water quality is minor; quality even improves due to lower waste water volumes that blend with fresh water resources.

The results obtained in this study could be used as a reference for regional water resources management in the JRB. The results also provide detailed information on spatially explicit effects that allow local policy makers to take matters in their own hand. As such, the model outcomes can also underpin the stakeholder discussions on distribution of water resources to support negotiations on water transfers, within and between basins.

Further validation exercises should strengthen the reliability of results obtained by the global climatic models (GCMs). Incorporation of local knowledge on water management that transcends

academic disciplines with practical solutions and on the ground reality further strengthens the water economy model's representation and its utility as decision support tool.

A. Appendix

See **Figures a1–a10**.

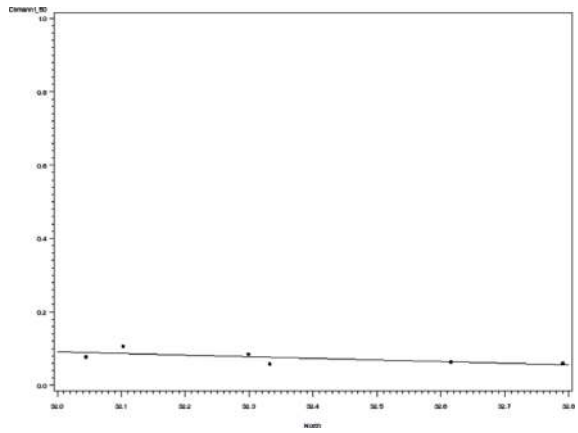

Figure a1. Relative future changes in precipiation against South-North gradient. Scenario: CanESM2 GCM, RCP2.6, time lapse 40 years.

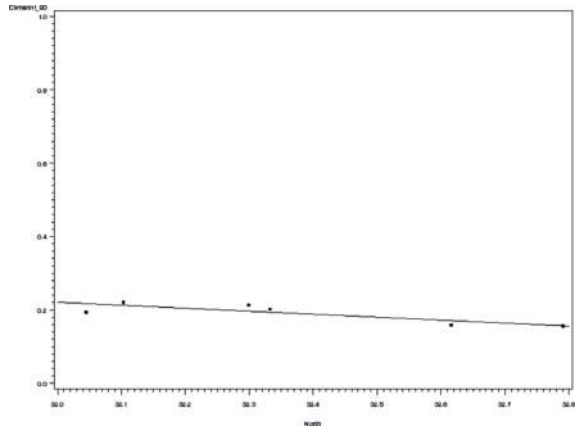

Figure a2. Relative future changes in precipiation against South-North gradient. Scenario: CanESM2 GCM, RCP2.6, time lapse 80 years.

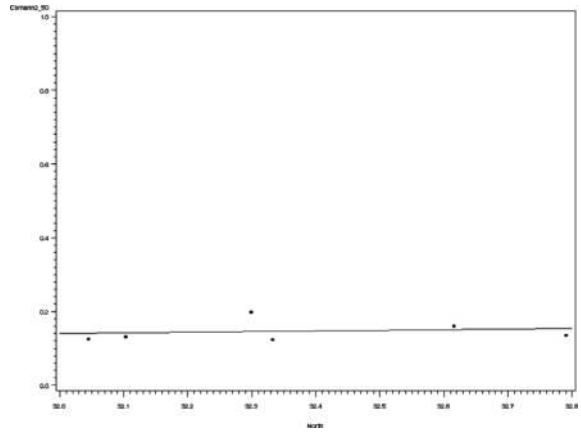

Figure a3. Relative future changes in precipiation against South-North gradient. Scenario: CanESM2 GCM, RCP4.5, time lapse 40 years.

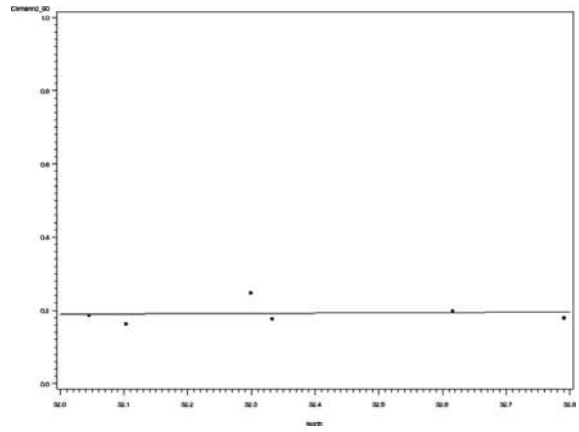

Figure a4. Relative future changes in precipiation against South-North gradient. Scenario: CanESM2 GCM, RCP4.5, time lapse 80 years.

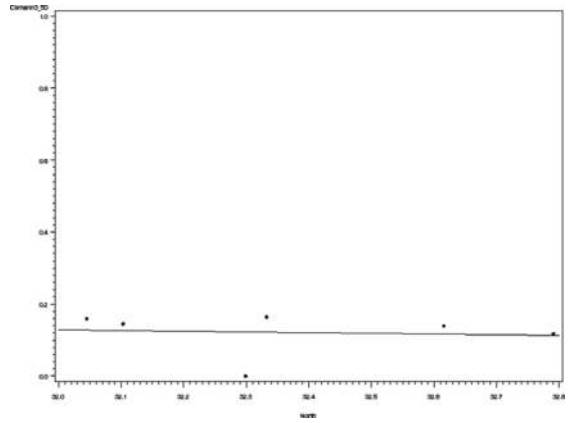

Figure a5. Relative future changes in precipiation against South-North gradient. Scenario: CanESM2 GCM, RCP8.5, time lapse 40 years.

http://dx.doi.org/10.5772/intechopen.80321

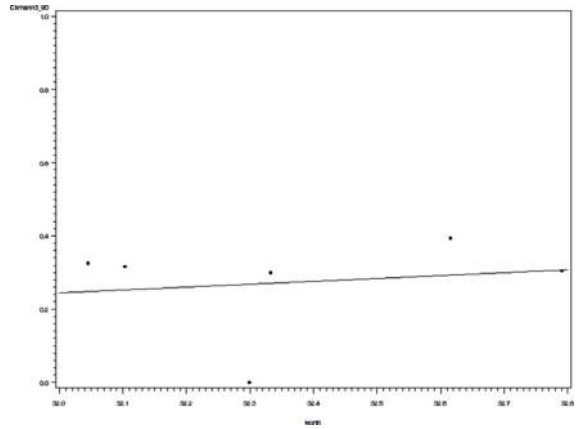

Figure a6. Relative future changes in precipiation against South-North gradient. Scenario: CanESM2 GCM, RCP8.5, time lapse 80 years.

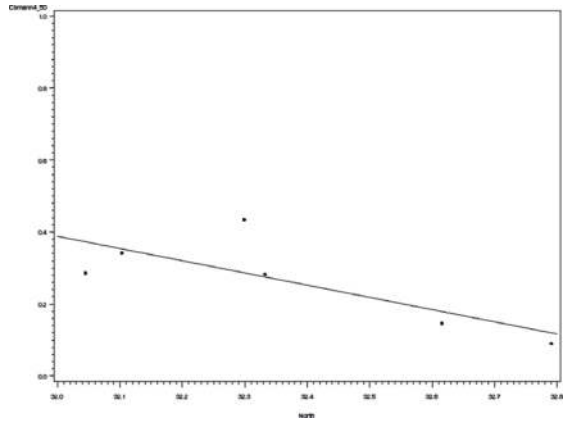

Figure a7. Relative future changes in precipiation against South-North gradient. Scenario: CGCM3 GCM, A1B, time lapse 40 years.

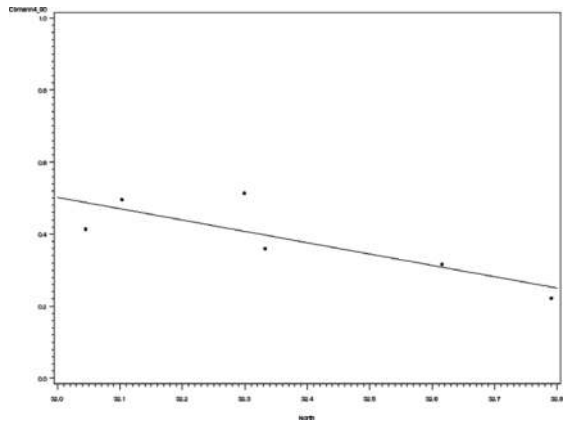

Figure a8. Relative future changes in precipiation against South-North gradient. Scenario: CGCM3 GCM, A1B, time lapse 80 years.

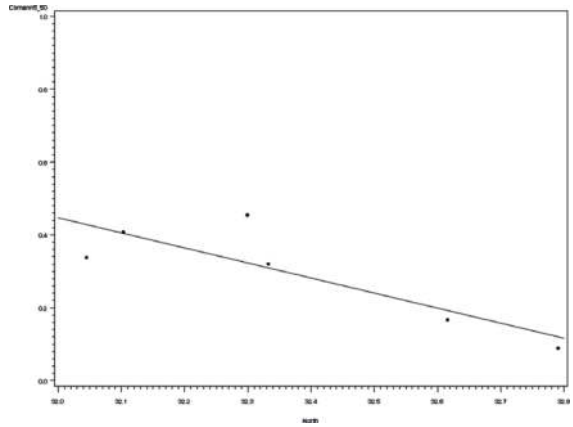

Figure a9. Relative future changes in precipiation against South-North gradient. Scenario: CGCM3 GCM, A2, time lapse 40 years.

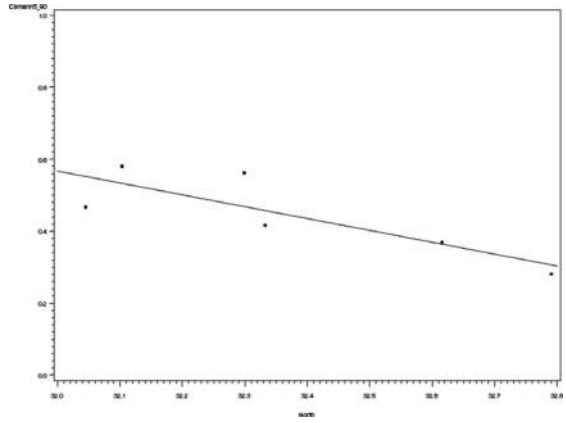

Figure a10. Relative future changes in precipiation against South-North gradient. Scenario: CGCM3 GCM, A2, time lapse 80 years.

Author details

Fayez Abdulla[1], Wim van Veen[2], Hani Abu Qdais[1], Lia van Wesenbeeck[2]* and Ben Sonneveld[2]

*Address all correspondence to: c.f.a.van.wesenbeeck@vu.nl

1 Civil Engineering Department, Jordan University of Science and Technology, Irbid, Jordan

2 Amsterdam Centre for World Food Studies, VU University, Amsterdam, The Netherlands

References

[1] WRI. World's 36 Most Water-Stressed Countries. Washington: World Resource Institute; 2013 http://www.wri.org/blog/2013/12/world%E2%80%99s-36-most-water-stressed-countries

[2] Abdulla FA, Eshtawi T, Assaf H. Assessment of the impact of potential climate change on the water balance of semi-arid watershed. Water Resources Management. 2009;**23**:2051-2068

[3] Selby J. Cooperation, domination and colonisation: The 'region a'-Palestinian joint water committee. Water Alternatives. 2013;**6**:1-24

[4] Wolf AT. Hydropolitics along the Jordan River; Scarce Water and Its Impact on the Arab—'Region a' Conflict, Vol. 99. United Nations University Press; 1995

[5] Ashok S, Jägerskog A. Emerging Security Threats in the Middle East: The Impact of Climate Change and Globalization. Rowman & Littlefield; 2016

[6] UN-ESCWA, BGR. Inventory of Shared Water Resources in Western Asia, Chapter 6, Jordan River Basin. Beirut: United Nations Economic and Social Commission for Western Asia; Bundesanstalt für Geowissenschaften und Rohstoffe; 2013

[7] Zeitoun M, Talhami M, Eid-Sabbagh K. The influence of narratives on negotiations and resolution of the upper Jordan River conflict. International Negotiation. 2013;**18**:293-322

[8] Flato G, Marotzke J, Abiodun B, Braconnot P, Chou SC, Collins W, et al. Evaluation of climate models. In: Stocker TF, Qin D, Plattner G-K, Tignor M, Allen SK, Doschung J, Nauels A, Xia Y, Bex V, Midgley PM, editors. Climate Change 2013: The Physical Science Basis. Contribution of Working Group I to the Fifth Assessment Report of the Intergovernmental Panel on Climate Change. Cambridge University Press; 2013. pp. 741-882. DOI: 10.1017/CBO9781107415324.020

[9] IPCC. Managing the risks of extreme events and disasters to advance climate change adaptation. In: Field CB, Barros V, Stocker TF, Qin D, Dokken DJ, Ebi KL, Mastrandrea MD, Mach KJ, Plattner G-K, Allen SK, Tignor M, Midgley PM, editors. A Special Report of Working Groups I and II of the Intergovernmental Panel on Climate Change. Cambridge, UK, and New York, NY, USA: Cambridge University Press; 2012. 582 pp

[10] Easterling DR, Evans JL, Groisman PY, Karl TR, Kunkel KE, Ambenje P. Observed variability and trends in extreme climate events: A brief review. Bulletin of the American Meteorological Society. 2000;**81**:417-425

[11] Gu H, Wang G, Yu Z, Mei R. Assessing future climate changes and extreme indicators in east and south Asia using the RegCM4 regional climate model. Clim. Change. 2012;**114**(2): 301-317. DOI: 10.1007/s10584-012-0411-y

[12] Abdulla F., H. Abu Qdais, A. Al-Shurafat, et al. (2016) Future changes in precipitation and maximum and minimum temperature using the statistical downscaling model (SDSM) in the trans-boundary Yarmouk River Basin

[13] van Veen W, van Wesenbeeck L, Merbis M, Sonneveld B. Towards concerted sharing: Development of a regional water economy model in the Jordan River Basin. Final Report. Centre for World Food Studies of the VU University Amsterdam; 2017

[14] Keyzer MA. Optimal calibration and control in a regional water economy model for the Jordan River basin. Working Paper under the project. Towards concerted sharing: Development of

a regional water economy model in the Jordan River Basin. Amsterdam, Netherlands: Centre for World Food Studies; 2015

[15] Merbis MD, Sonneveld B. Construction of water response functions in the Jordan River basin. Working paper under the project. Towards concerted sharing: Development of a regional water economy model in the Jordan River Basin. Amsterdam, Netherlands: Centre for World Food Studies; 2016

[16] McKinney W. Data structures for statistical computing in Python. In: Proceedings of the 9th Python in Science Conference. 2010. pp. 51-56